EXPERIMENTS AND ANALYSIS OF THE LIMIT STRESSES
OF A MAGNETORHEOLOGICAL FLUID

Wojciech HORAK* , **Barbara STĘPIEŃ*** , **Bogdan SAPIŃSKI****

*Department of Machine Design and Technology, Faculty of Mechanical Engineering and Robotics,
AGH University of Science and Technology, Al. Mickiewicza 30, 30-059 Kraków, Poland
**Department of Process Control, Faculty of Mechanical Engineering and Robotics,
AGH University of Science and Technology, Al. Mickiewicza 30, 30-059 Kraków, Poland

horak@agh.edu.pl, bstepie@agh.edu.pl, deep@agh.edu.pl

Abstract: This paper presents the results of a rheological test of a commercial magnetorheological (MR) fluid (MRF-132DG). The research includes the problem of measuring and interpreting limit stresses under conditions close to the magnetic saturation of the fluid. Four different limit stresses were determined, two related to the yield point and two related to the flow point. Methods for determining limit stresses, especially due to excitation conditions, were also analysed. The aim of this study is to determine the effect of selected parameters on the values of limit stresses of the selected MR fluid. An additional objective is to highlight the problems of defining and interpreting individual limit stresses in MR fluids, particularly in the context of selecting the values of these stresses for the purpose of modeling systems with MR fluids.

Key words: magnetorheological fluid, yield stress, flow stress, dynamic properties, rheology

1. INTRODUCTION

Among smart materials, there is a group of fluids that are sensitive to changes in the magnetic field. For application purposes, controlling the material's properties with changes in the magnetic field is a convenient and effective method. Nowadays, magnetorheological (MR) fluids are widely applied in systems with controllable characteristics. They are suspensions of magnetic particles in a non-magnetic base fluid. Additives against particle agglomeration and sedimentation are also used as additional components. When the MR fluid is exposed to a magnetic field, the structure of the suspension changes, causing changes in its rheological properties. This reaction is immediate and fully reversible [1-6]. Depending on the configuration of the MR fluid flow and the orientation of the magnetic field acting on it, there are four work mode types that can be distinguished: the flow, shear, squeeze and pinch modes.

In the flow mode (also known as the valve mode), fluid flow is due to the pressure difference. The surfaces of the working geometry are stationary, and the magnetic field is usually oriented perpendicular to the flow direction. The flow mode is found in dampers, shock absorbers and servo valves [7–9].

The second mode of operation is the shear mode, in which the flow of the fluid is achieved by the movement of one or more surfaces interacting with the MR fluid, when the magnetic field is perpendicular to the flow (surface movement) direction. This mode is characteristic for brakes and clutches [10, 11].

In the squeeze-flow mode, the MR fluid is located between the surfaces approaching each other, with the magnetic field induction

vector usually parallel to the direction of surface motion and perpendicular to the MR fluid flow direction. This flow mode is observed in some vibration damping devices and low power consumption valves [12–16].

In recent years, a new pinch mode, mainly used in valves, has been proposed [9, 10]. It shares features with the flow mode, but the main difference is the presence of a non-uniform (region of highly concentrated) magnetic field.

For devices working with MR fluids, the key aspect is a change in the apparent viscosity, observed as the ability to transition from a fluid state to a solid consistency. Control in the range of viscosity change is used primarily in vibration dampers [17] and controlled (measuring) brakes, while the control of fluid yield or flow stresses is particularly important for holding brakes [18], clutches [19] and valves [20, 21].

In the present work, attention is paid to the problem of limiting stresses. The main factors that affect the ability to achieve a suitable value of this parameter are the magnetic field strength acting on the fluid and the composition of the MR fluid, especially the quantity, size and magnetic parameters of the ferromagnetic particles used to prepare the suspension [5, 22–26].

As noted earlier, the value of limit stresses in MR fluids is crucial for the operation of certain devices. However, it should be emphasised that for MR fluids, as in other substances with complex rheological properties, the process of transition to the state of plastic deformation is a multifaceted issue. For MR fluids, it is possible to observe the occurrence of the 'two-step yielding' phenomenon, i.e. a two-step transition from a solid to a fluid-like state, due to increasing stress or strain. In this case, two limit stresses can be distinguished. The first, viz. the yield point, refers to the

onset of breakage of the fluids' internal structure, while the second, i.e. the flow point, refers to the rupture of the substance's internal integrity.

The aim of this study is to evaluate the conditions for the occurrence of limiting stresses that determine the start of flow of a selected MR fluid. The tested fluid is commercially available and has been applied in vibration dampers and brakes. The scope of the study was limited to high values of magnetic induction, so the results relate to conditions close to the saturation of the tested fluid.

2. METHODS OF DETERMINATION OF THE LIMIT STRESSES

The limit stresses of plastic materials can be defined as the critical amount of applied stress below which it will not flow, but it is a conventional concept and depends on the conditions and method of its determination. It can be distinguished as two forms of that stress: the yield stress is the load that limits the elastic behaviour of the material and the flow stress, and it is usually understood as the point of occurrence of a go-no-go behaviour. The second limit load is commonly used for MR fluids. It is usually given as a material constant.

One of the main criteria of the flow or yield behaviour occurring is the time and (due to the method of measurement) the method followed to control the test, i.e. the controlled shear rate (CSR) or the controlled shear stress (CSS) [27, 28].

Among the main methods used to determine the yield stress is reading the stress curve where the curve intersects the shear stress axis (τ_Y in Fig. 1a). This method is simple, but not very accurate, and can only be used to estimate the value of the flow limit. Attention should be paid here to the method of applying excitation. It is recommended to perform the measurement with a CSS, so that the stress that initiates the flow can be obtained with greater accuracy.

Due to the complexity of the material's transition through the range of the onset of flow, a useful method is to use mathematical models that approximate the points that determine the flow curve. The yield stress is extrapolated as the shear stress corresponding to a shear rate equal to zero. For MR fluids, the most commonly used models are as follows: Bingham (τ_{YB} in Fig. 1a), Herschel–Bulkley, Casson, Sisko, Robertson–Stiff and bi-plastic [29, 30].

The yield stress can be determined as the value of the shear stress at the lowest shear rate (τ_Y in Fig. 1b) or as the shear stress corresponding to a low shear rate, conventionally 0.01 s^{-1} (τ_F in Fig. 1b). Using this method, it is advantageous to represent the flow curves on a double logarithmic scale.

In the method shown in Fig. 1c, a straight line is fitted to low shear rates, and the last point belonging to this straight line is the yield stress (τ_{Y1}). In practice, there is an acceptable deviation of the point value of the fitted straight line, e.g. ±5%. This method can be further developed by fitting a second straight line to points corresponding to high shear rates. The flow limit is then defined as the intersection point of the two straight lines (τ_{Y2}).

However, the above methods do not take into account the occurrence of viscoelasticity, which is a major simplification in the case of MR fluids. In the low-strain range, there can be high elastic stresses in MR fluids [31].

Viscoelasticity can be observed in dynamic mechanical analysis (DMA) tests. Using this method, it is possible to determine the storage modulus G' expressing the elastic properties of the fluid

and the loss modulus G'' related to viscosity behaviour (Fig. 1d). Yield stress is defined as the value of shear stress at the end of the linear viscoelastic range (LVE) (τ_Y). In another approach, it is the shear stress for which the G' curve leaves the plateau region. In this concept, it becomes important to assume an appropriate criterion for the occurrence of the end of the LVE range. Typically, the case where there is a 5% or 10% change in G' is taken as the end of the LVE [32].
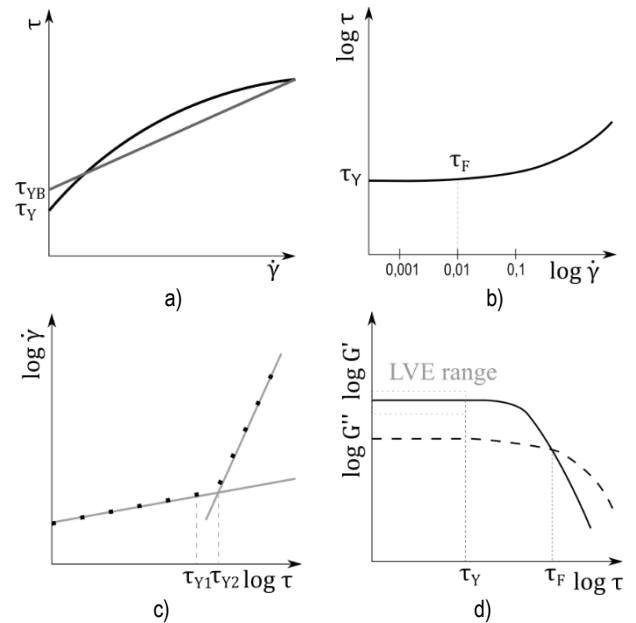

Fig. 1. Methods of determining limit stresses: (a) as the intersection of the flow curve with the stress axis (τ_Y), the Bingham model yield stress (τ_{YB}); (b) as the initial values of the shear stress (τ_Y) on a double logarithmic scale and as the value obtained for a low shear rate of 0.01 s^{-1} (τ_F); (c) using the linear function approximation method (τ_{Y1}, τ_{Y2}); and (d) as the end of the LVE range (τ_Y) and intersection of G' and G'' (τ_F)

Furthermore, the DMA method also allows the flow stress (τ_F) to be determined. This is the stress corresponding to the intersection of the G' and G" curves. It should be emphasised here that this approach is conventional and uses the typical course of variation in the properties of fluids.

The stress–strain range between the yield point and the flow point is called the yield or the yield/flow transition zone. In this range, $G'>G''$ is still observed, indicating that the fluid exhibits gel-like behaviour. However, there is a dramatic loss of its elastic properties. From the physical side, this behaviour can be explained by changes in the microstructure of MR fluids. All possible elastic deformations have already occurred, and irreversible deformations associated with the degradation of the fluid's internal structure have begun. All these facts contribute to the complexity of the phenomena observed during the transition of MR fluids from the resting state to elastic and plastic deformation.

3. TESTED SAMPLE

The tests were conducted on LORD's MRF-132DG (Cary, North Carolina, USA) commercial fluid. The manufacturer specifies that the fluid is dedicated to shear and valve-mode operation [33].

Wojciech Horak, Barbara Stępień, Bogdan Sapiński
Experiment and Analysis of the Limit Stresses of Magnetorheological Fluid

DOI 10.2478/ama-2022-0049

Tab. 1. Basic properties of MRF-132DG [33]

Property	Value
Density	2.95–3.15 g/cm^3
Dynamic viscosity at 40°C	0.112±0.02 Pa·s
Solid content	80.98 wt.%
Flash point	>150°C
Operating temperature	–40°C to 130°C

The essential properties of the tested fluid, as declared by the manufacturer, are listed in Tab. 1. One of the key features of the tested fluid is the low value of dynamic viscosity under zero magnetic field and the high value of yield stress in the presence of a magnetic field.

Numerous papers that have addressed this fluid's properties cover the range of low and medium magnetic field induction values – usually up to about 400 mT [34-36]. With respect to higher values of the magnetic field, in a previous work [30], studies with values up to 600 mT were carried out. In all these works, the properties of the fluids were related to the well-known Bingham, Herschel–Bulkley and power rheological models, which obtained a fluid stress of 12–16.5 kPa (at B = 300 mT). However, a full evaluation of the ability of this fluid to obtain high shear stresses requires the performance of tests in the higher range of magnetic field. As shown in Fig. 2, the tested MR fluid allows yield stresses of >48 kPa to be obtained, which occurs at a magnetic induction of about 1 T.
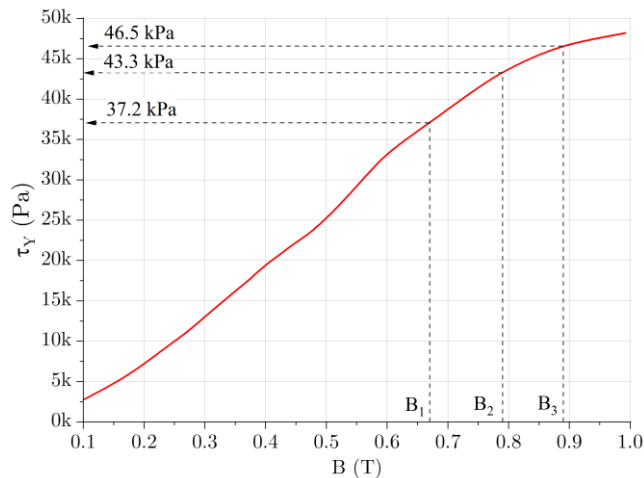

Fig. 2. Yield stress (τ_Y) vs. magnetic induction (B) of MRF-132DG. Based on LORD Corporation's datasheet [33]

The results of the analyses discussed in the present work refer to three values of magnetic field induction. They are marked in Fig. 2 with dashed lines, and the corresponding values of the yield stresses are given. As can be seen, the analysed values of magnetic induction cover the upper range of expected shear stresses.

4. EXPERIMENTS

The experiments were carried out on an MCR-301 rotational rheometer with an MRD180/1T cell, dedicated to conducting tests in the presence of a magnetic field. A plate–plate geometry with the diameter of d = 20 mm was used, and the height of the measuring gap was h = 0.6 mm, for which the sample volume was V = 200 µl. All tests were carried out under thermal stabilisation conditions of t =25°C.

The source of the magnetic field in the measuring cell was an electromagnet, powered from an external DC power supply. For the purpose of this work, the power supply and its control system were modified, which allowed the setting of higher-than-nominal current values ranging from 0 to 5 A to 0 to 6 A. After the modification, the values of magnetic field induction in the working gap of the rheometer were measured. Fig. 3 shows the $B=f(I)$ curves for the modified system. The tests were carried out for three values of electromagnetic current $I_{1,2,3}$ = 4/5/6 A, which correspond to the magnetic field induction $B_{1,2,3}$ = 670/790/890 mT.
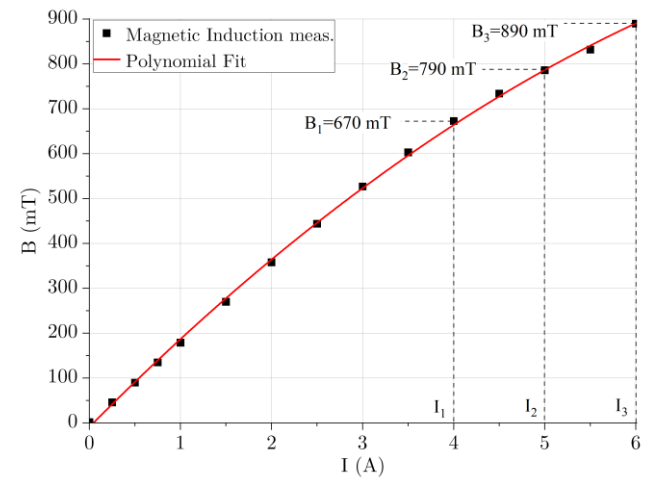

Fig. 3. Magnetic induction (B) vs. current (I) for the modified rheometer measuring cell supply system

The pivotal tests were preceded by preliminary studies, which included Magneto Sweep experiments. This test consists of applying a linearly increasing magnetic field induction during the measurement. It also allows an overall evaluation of the response of the test sample to the application of the magnetic field. Two test types were performed:

- Magneto Sweep at rotational excitation (I = 0–6 A, (B = 0–890 mT), $\dot{\gamma}$ = 0.1/1/10/100 s^{-1});
- Magneto Sweep at oscillatory excitation (I = 0–6 A (B = 0–890 mT), f = 1/10/25 Hz, γ = 0.1%/1%/100%).

The aim of the preliminary tests was to determine the response of the tested fluids to different types of excitation over a wide range of applied magnetic field. The research investigated the effect of the strain value and rate.

The primary research phase included three types of research:

- Rotational CSSt (controlled shear strain) tests
- Rotational CSS tests
- Dynamic DMA (controlled shear strain) tests

The scope of the tests included three values of magnetic induction ($B_{1/2/3}$=670/790/890 mT), three values of the stress increase rate ($v_{1/2/3}$=2.5/5/10 s) in the range 3–30 kPa and three oscillation test frequencies ($f_{1/2/3}$= 1/10/25 Hz). The results of each test were used as input data to determine the corresponding values of each limit stress.

5. RESULTS AND DISCUSSION

5.1. Magneto Sweep - rotational

The results of shear stress measurements under increasing magnetic field induction at different shear rates are shown in Fig. 4. In the lower range of magnetic induction (<400 mT), the effect of shear rate is relatively small, while higher stress occurs at higher shear rates. This is typical behaviour due to the correlation between the apparent viscosity of the fluids and shear stress. As magnetic induction increases, this trend reverses. The change point of this trend occurs for the magnetic induction B =300 mT. The lower the shear rates, the higher are the stress values obtained. In the extreme case, the shear stress for $\dot{\gamma}$ = 0.1 s^{-1} is 40% higher than when measured for $\dot{\gamma}$ = 100 s^{-1} (25 vs. 35 kPa). The explanation for this behaviour is that lower shear rates promote the preservation of greater internal integrity of structures inside MR fluids, which results in higher deformation resistance.
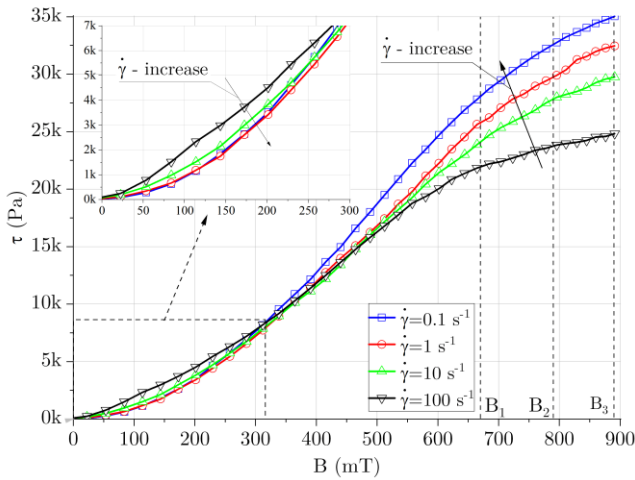

Fig. 4. Shear stress (τ) vs. magnetic induction (B) at rotational excitation

5.2. Magneto Sweep – oscillatory method

Fig. 5 shows the results of measuring shear stress under oscillatory excitation. The tests were performed for three values of strain amplitude. For γ=0.1%, relatively low stress values were obtained, with no change from about B =300 mT onwards. With such a small degree of sample deformation, it was not possible to obtain higher stresses. Excitation levels of 1% and 100% resulted in correspondingly higher stress values. With 1% strain, a decrease in the stress increment in the magnetic induction range greater than B_1 is observed, while for γ = 100%, the stress increases approximately in proportion to the increase in the applied magnetic field induction. Thus, it can be assumed that in the case of 0.1% and 1% strain, a sort of saturation state has been obtained, for which a further increase in magnetic induction does not lead to an increase in stress.

In Fig. 5, the stress ranges corresponding to the three values of magnetic induction, for which analyses were carried out in the following part of the work, are indicated using curly brackets. The obtained results show that the differences in the measured shear stress, which depend on the oscillation frequency, are not significant and are within ±1 kPa.
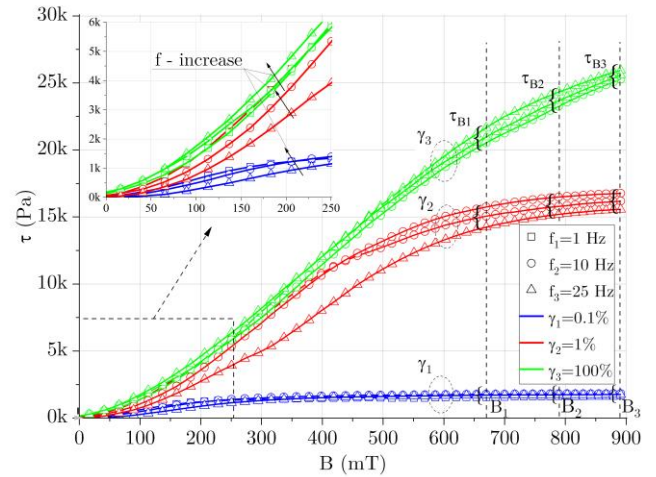

Fig. 5. Shear stress (τ) vs. magnetic induction (B) at oscillatory excitation

5.3. Strain–shear stress relation

Fig. 6 shows the results of the shear stress measurements under controlled strain (γ = 0.01%–100%) and three values of magnetic field. The measurement simulates the method of excitation that occurs in MR fluid systems operating with displacement control.
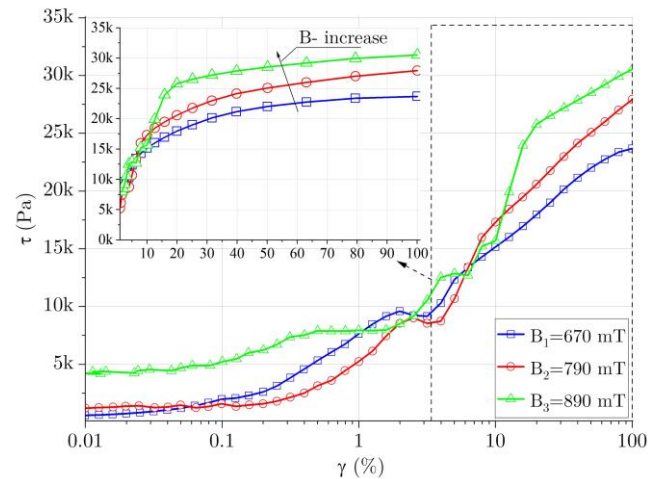

Fig. 6. Shear stress (τ) vs. strain (γ) obtained from controlled strain measurements

In the very low strain range (γ<0.1%), the stress values depend very slightly on the strain, which is visible as a plateau region in the first part of the curves. The second characteristic value that can be indicated is γ>10%, for which the behaviour of the fluids is consistent with typical rheological models. From the perspective of this paper, an important aspect is the analysis of the transition range (strain from 0.1% to about 1%), with this range including the excitation at which the fluid starts to flow, i.e. yield stress and flow stress.

Fig. 7 shows the result of the stress measurement, but in this case, the test was carried out with CSS. This is the recommended method for determining limit stresses in fluids. The test was based on logarithmically increasing the stress in the range of 3–30 kPa and observing the sample deformation. The measurements were repeated for three stress increase rates v = 2.5/5/10 s (which

Wojciech Horak, Barbara Stępień, Bogdan Sapiński
Experiment and Analysis of the Limit Stresses of Magnetorheological Fluid

DOI 10.2478/ama-2022-0049

correspond to the gradients of stress change, respectively, Δτ=10.8/5.4/2.7 kPa·s⁻¹). The results shown in Fig. 7 were used to determine the flow stress (τ_Y).

In the inset in Fig. 7, the arrows indicate the direction of increase in the stress gradient. For the two lower values of magnetic induction, the increase in the rate of stress change results in an increase in the obtained stresses, while with B_3, the trend is reversed. While the behaviour observed for B_3 is consistent with the previous results (see Fig. 4), the measurement results for B_1 and B_2 can be explained as the effect of the measurement duration. With a lower magnetic field, the shorter test time resulted in lower stress values. This may result from the fact that, at lower values of the magnetic field, the MR fluid structure was not as strong as it was in the higher one. This thread requires further research. From the point of view of this work, it is important to determine the flow stress, which in the case of this measurement can be determined as the break point of the curve.
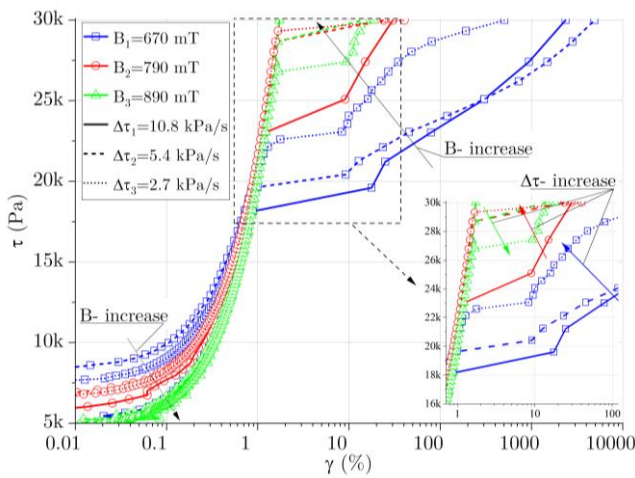

Fig. 7. Shear stress (τ) vs. strain (γ) obtained from controlled shear stress measurements (Solid, dashed and dotted lines represent Δτ = 10.8/5.4/2.7 kPa s⁻¹, respectively)

It should be noted that, in the case of the highest analysed magnetic field induction, at the lowest rate of stress increase, no fluid flow was obtained. This indicates that the flow stress for this measurement is >30kPa.

5.4. Limit stresses

5.4.1. Rotational test-stress ramp

Based on the data from CSS-type measurements, the values of the yield stress (τ_{CSS}) were determined for different gradients of stress increase. The results are shown in Fig. 8. The gradient of stress increase can significantly affect the value of the limit stress. This is particularly visible at lower values of magnetic field induction, which may result from the aforementioned duration of the measurement.

The inset in Fig. 8 shows the average values of flow stress calculated from the measurement results for different gradients of stress increase. The extreme values (minimum/maximum [min/max]) are marked using the error bar. For B_1 = 670 mT and B_2 = 790 mT, the change in τ_{CSS} from the average value is approx-

imately 12%, while for B_3 = 890 mT, it is <4%. Since, for the measurement of B_3 and $Δτ_1$, the limiting stress was not reached, the yield stress value of 30 kPa was used for the analysis.
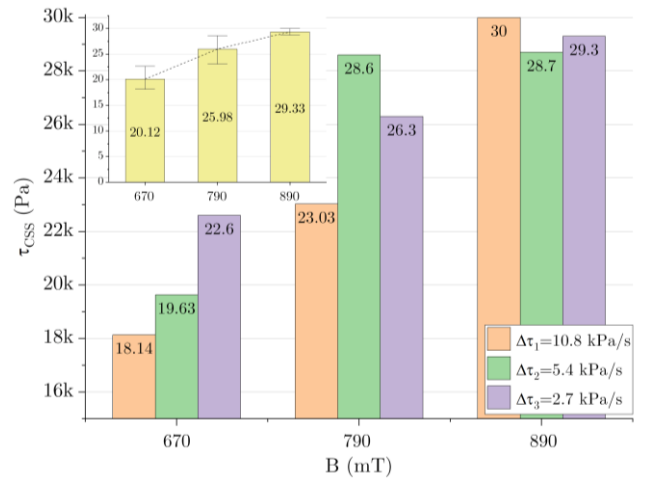

Fig. 8. Yield stress (τ_{CSS}) vs. magnetic induction (B) obtained from controlled shear stress measurements

5.4.2. Oscillatory test

Fig. 9 summarises the results of the dynamic (oscillation) measurements. The tests were carried out for three values of magnetic induction with a logarithmic strain ramp γ = 0.01%–1,000% and three oscillation frequencies ($f_{1,2,3}$ = 1/10/25 Hz). Thus, for a strain equal to 100%, the shear rate will be 6.3, 63 and 157 s⁻¹, respectively.

Due to the quite high values of magnetic induction (starting from B =690 mT) and a wide range of deformation, reaching very small deformation (up to 0.01%), high values of the elastic modulus (G') were obtained in all measurements and a distinct LVE range was observed. The end of this, for all analysed cases, falls under a deformation of about 1%.
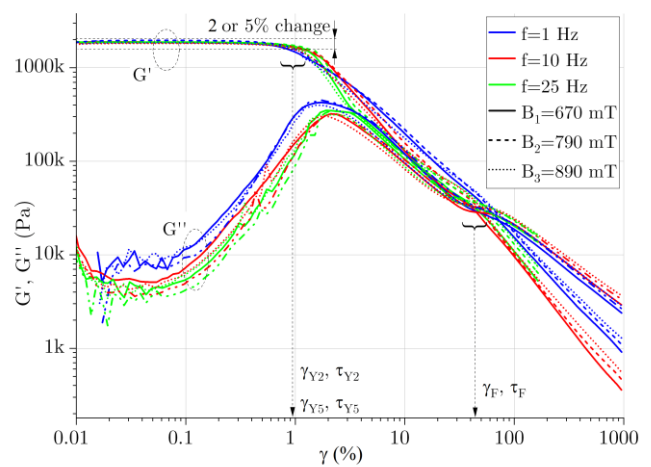

Fig. 9. Storage (G') and loss (G'') modulus vs. strain (γ)

The data shown in Fig. 9 were used to determine yield and flow stresses. In the case of yield stress, two values were established corresponding to two criteria for its determination. It was

arbitrarily assumed that the stress that occurs when the elastic modulus changes by 2% or 5% would be considered as the value of these yield stresses. The notation for these parameters was adopted as $\tau_{Y2\%}$ and $\tau_{Y5\%}$.

On the basis of the discussed results of dynamic tests, the flow point was also determined as the stress corresponding to the balance point $G'=G'$ and denoted as τ_F. Fig. 9 symbolically denotes the discussed ranges and parameters (stresses and corresponding strains) using dashed lines.

Fig. 10 summarises the limit stresses determined from the dynamic tests. As expected, the yield stresses $\tau_{Y2\%}$ and $\tau_{Y5\%}$ have a similar course. It should be emphasised that increasing the tolerance in the method of determining the yield stress from 2% to 5% results in an increase in the value of this stress by an average of 42% (min: 33%; max: 51%). This result indicates that the choice of the yield stress criterion has a significant effect on its value.

Analysing the effect of the excitation frequency on yield stresses ($\tau_{Y2\%}$, $\tau_{Y5\%}$), it can be observed that yield stress increases as the deformation rate of the specimen increases. This is especially evident when increasing the frequency from 1 Hz to 10 Hz. On the contrary, the opposite trend is seen in the case of flow stress (τ_F). Note that the nature of the flow stress variation is similar both qualitatively and quantitatively to τ_{CSS} (Fig. 8).
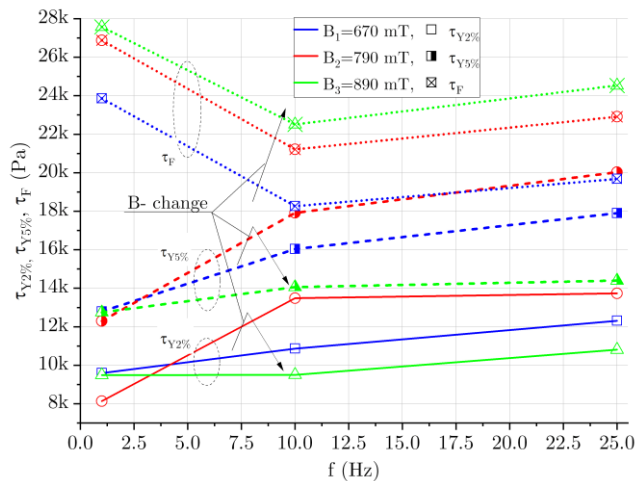

Fig. 10. Yield stresses ($\tau_{Y2\%}$, $\tau_{Y5\%}$) and flow stress (τ_F) vs. frequency (f) obtained from oscillatory tests

Furthermore, Fig. 11 shows the strain values corresponding to the values of the respective limit stresses. For the yield stress (τ_Y), an increase in excitation frequency results in an increase in the strain at which the flow occurred, while for the flow stress (τ_F), a significant reduction in the strain corresponding to the flow is observed for tests performed at higher frequency.

Thus, an increase in the rate of the sample deformation, in the case of yield stress, causes an increase in the degree of deformation at which it occurs, as well as the corresponding stress. In the case of flow stress, the trend is the opposite.

The test method used makes it possible to observe the behaviour of the samples in the range between yield stresses (τ_Y) and flow stresses (τ_F). To represent the behaviour of the test sample before flow occurs, Fig. 12 shows plots of the variation of the damping ratio ($tan(\delta) = G''/G'$) as a function of the applied strain.

The characteristic value for the discussed analysis is $tan(\delta) =1$, which corresponds to the flow point of the tested sample. As shown in Fig. 11, the deformation corresponding to the

yield stress (τ_Y) is in the range of 0.4%–1.25% and corresponds to the initial phase of the graphs shown in Fig. 12. In this range of deformation, there is a high modulus of elasticity (G'') with relatively low values of the loss modulus (G'). A rapid change in the ratio of G' and G'' is observed at strains of about 3%–5%. In this range, the maximum value of the loss modulus is exceeded, and a sharp decrease in the elastic modulus begins (compare with Fig. 9).
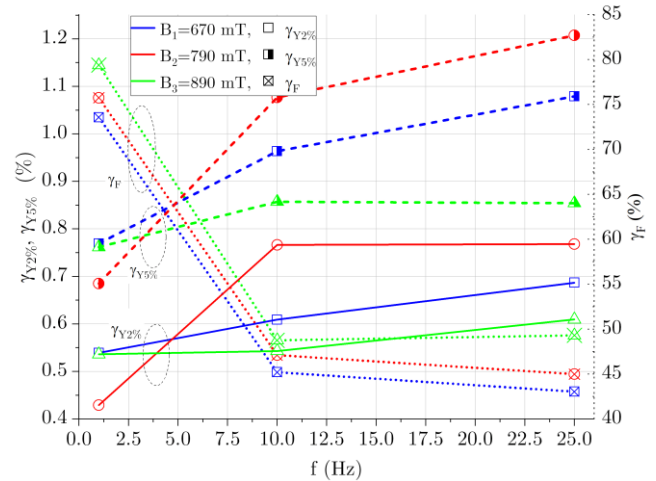

Fig. 11. Yield strain ($\gamma_{2\%}$, $\gamma_{5\%}$) (left axis) and flow strain (γ_F) (right axis and dashed lines) vs. frequency (f) obtained from oscillatory tests

This corresponds to the non-linear range of $tan(\delta)$ variation and ends in the deformation range of 30%–40%, which corresponds to the approach of the values of individual stiffness modules. In the discussed diagram, the ranges of deformation corresponding to individual limit stresses are marked with the use of curly brackets.
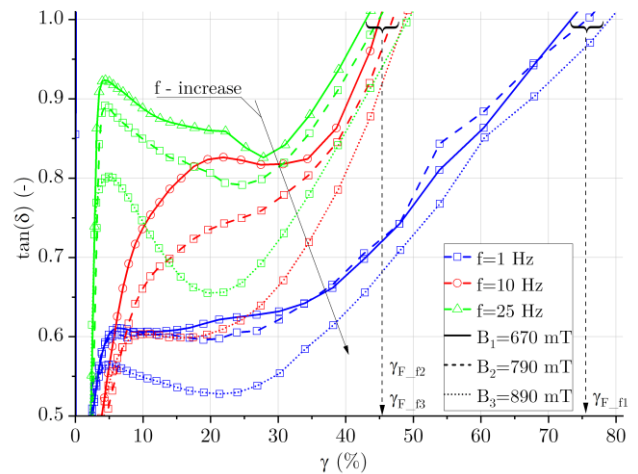

Fig. 12. Damping factor ($tan(\delta)$) vs. strain (γ) in the post-yield region

From an application perspective, it is important to evaluate the variation of the shear stress in terms of excitation after the yield stress (τ_Y) and before the flow stress (τ_F). For this purpose, in Fig. 13, the relation of shear stress to the damping coefficient $tan(\delta)$ is shown.
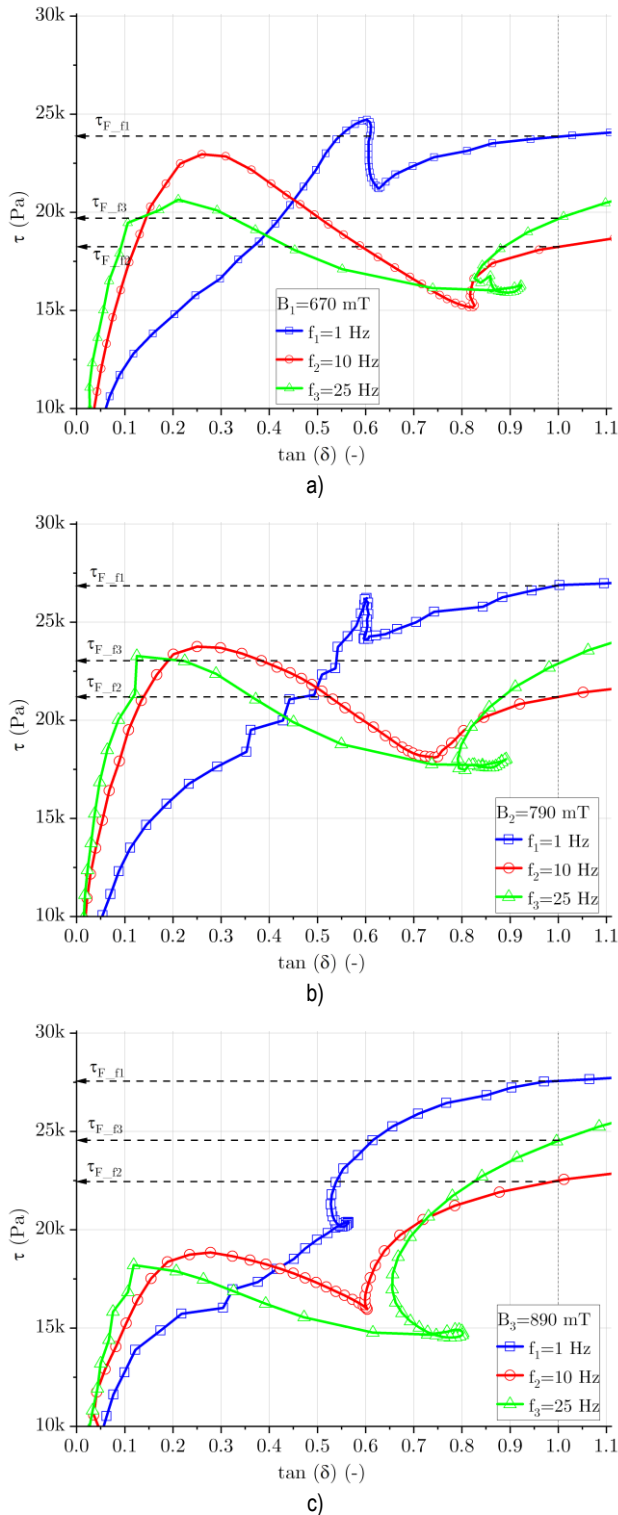
Wojciech Horak, Barbara Stępień, Bogdan Sapiński
Experiment and Analysis of the Limit Stresses of Magnetorheological Fluid

DOI 10.2478/ama-2022-0049

Fig. 13. Shear stress (τ) vs. damping factor ($tan(\delta)$) in the post-yield region for variable magnetic induction (a) B_1 = 670 mT; (b) B_2 = 790 mT; and (c) B_3 = 890 mT

In the diagrams, the stress values corresponding to the flow stress (τ_F) are marked with arrows. For the lowest magnetic field induction (B_1), the shear stress value in the range of $tan(\delta)<1$ is higher than the flow stress (τ_F). Therefore, it is possible that the stress in the fluid exceeds the flow stress value before the fluid flows. In the transient region, there are strong non-linear relationships between the dynamic properties of the tested MR fluids and

stress. In particular, at higher excitation frequencies and higher values of magnetic induction, there is a tendency to 'loop' the discussed relationship, i.e. before reaching the flow stress (τ_F), there is a sharp decrease in $tan(\delta)$, which is visible on the graphs as a collapse or looping in the curves.
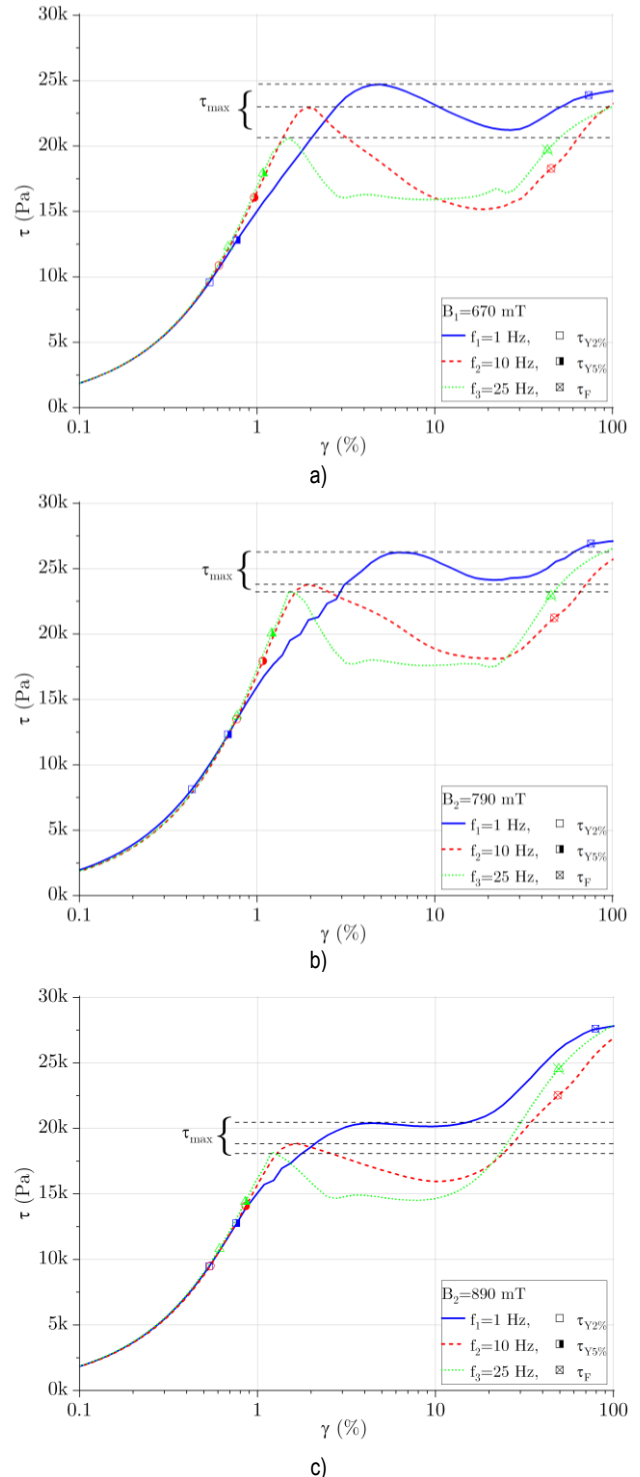
5.4.3. Analysis of the limit stresses

Fig. 14. Shear stress (τ) vs. strain (γ) for variable magnetic induction: (a) B_1 = 670 mT; (b) B_2 = 790 mT; and (c) B_3 = 890 mT (The open marks correspond to $\tau_{Y2\%}$, half-coloured regions correspond to $\tau_{Y5\%}$ and the crossed marks correspond to τ_F)

Fig. 14 summarises the curves of stresses as a function of strain, determined from oscillatory measurements. The points corresponding to the previously determined limit stresses are marked on the curves. As discussed earlier, the non-linearities can be seen as stress fluctuations in the transient region. After reaching the yield stress (τ_Y), there is a further increase in stress in each of the analysed cases, passing into the 'plateau' range and then increasing at the strain preceding the flow stress (τ_F) (compare Fig. 12).

It should be noted that, similar to what was observed in the context of *tan(δ)*, at lower values of the magnetic field, the stresses in the transition range exceed the values of the flow stress (τ_F). Naturally, this is related to the measurement method in which the controlled stress allowed this to occur. This behaviour is important for all systems operating under controlled deformation. In the context of the design of such systems in particular, it is to be expected that, at sufficiently low strains, it is possible for stresses to occur higher than those derived from the flow stress determined by the CSS method, by CSR or from dynamic tests.

To summarise the results of the determined limit stresses, Fig. 15 shows all of the results as a bar graph. As can be seen, the highest limit stress values were obtained from the CSS test method (τ_{CSS}), but are close to the flow stress (τ_F) determined from oscillatory measurements. This is an expected result, as dynamic tests allow detection of the beginning of changes in the MR fluid structure at an earlier stage of internal integrity loss. In the context of the yield stress (τ_F), the strong effect of the excitation frequency on the value of the boundary stress is distinguishable.

To highlight the complexity of interpreting limit stresses for MR fluids, Fig. 16 shows the average value of all limit stresses (both yield and flow states) obtained for three values of magnetic field induction. The bars correspond to the average value, and the points correspond to the values of individual measurements, while the box represents the range of stress variation.
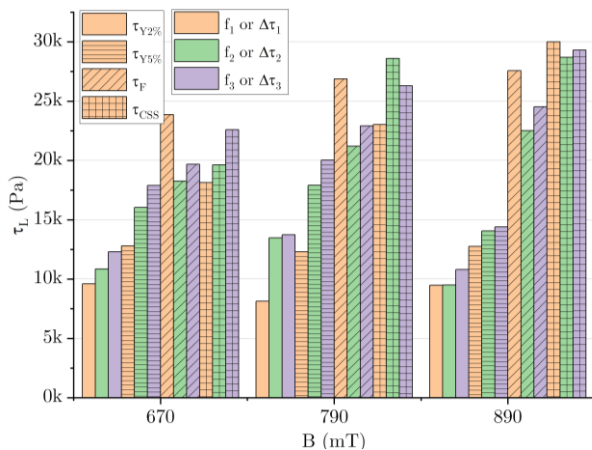

Fig. 15. Limit stresses (τ_L) vs. magnetic induction (*B*)

As can be observed, the criterion for determining the limit stress and the conditions of measurement have a significantly stronger influence on the obtained value than the value of magnetic field induction. Therefore, for the design and analysis of systems with MR fluids, for which the value of limit stresses is crucial, it is important to evaluate the criterion for determining a specific limit stress.

It is noteworthy that the stresses declared by the manufacturer (see Fig. 2) were not obtained in any of the performed measurements. This may be related to the difference between the test

methods and the parameters presented in the present work and those used by the manufacturer. However, it should be noted that, in the case of the highest value of the magnetic field induction value (*B* = 790 mT), the difference reaches 55% (from 46.5 kPa declared by the manufacturer; 30 kPa was obtained instead). However, good correspondence was obtained with the results of some previous works [34–37] related to the study of MRF-132DG fluids, in the range of low magnetic field induction, where the expected shear stresses are at the level of several kilopascals.
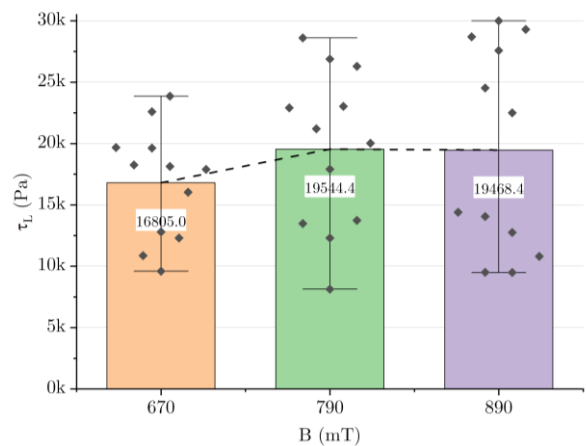

Fig. 16 Limit stresses (τ_L) vs. magnetic induction (*B*) (bar: mean limit stress, dots: each measurement, error bar: min–max range)

6. CONCLUSION

The paper presents an analysis of the variation of limit stresses of the MRF–132DG fluid, under a magnetic field value close to the saturation state.

The complexity of the problem concerning the methodology for determining limit stresses is shown. The values of the yield (τ_Y) and the flow (τ_F) stresses are significantly dependent on the deformation rate. However, for yield stress, an increase in the deformation rate results in an increase in its value, whereas for flow stress, the trend is the opposite.

Furthermore, it has been shown that the rate of stress change can significantly affect the value of the limit stresses.

The selection of the value of the tolerance change *G'* as an indicator of yield stress occurrence is of significant importance for the obtained stress values. A change from 2% to 5% results in an increase in yield stress of an average of 42%.

It has also been shown that adopting an appropriate value of the limiting stresses suitable for a given application can be crucial in predicting how it will perform. Under specific operating conditions (such as very small strains), taking into account the relation *τ=f(B)* as a simple function, without considering the conditions for measuring this parameter, may be an oversimplification.

REFERENCES

1. Khajehsaeid H, Alaghehband N, Bavil PK. On the yield stress of magnetorheological fluids. Chemical Engineering Science. 2022;256:117699.
2. Kumar M, Kumar A, Bharti RK, Yadav HNS, Das M. A review on rheological properties of magnetorheological fluid for engineering components polishing. Materials Today: Proceedings. 2022;56(3):A6-A12.

3. de Vicente J, Klingenberg DJ, Hidalgo-Alvarez R. Magnetorheological fluids: a review. Soft Matter. 2011;7:3701-3710.
4. Yang J, Yan H, Wang X, Hu Z. Enhanced yield stress of magnetorheological fluids with dimer acid. Materials Letters. 2016;167:27-29.
5. Asiaban R, Khajehsaeid H, Ghobani E, Jabbari M. New magnetorheological fluid with high stability: Experimental study and constitutive modelling. Polymer Testing. 2020;8:106512.
6. Kubík M, Válek J, Žáček J, Jeniš F, Borin D, et al. Transient response of magnetorheological fluid on a rapid change of magnetic field in shear mode. Scientific Reports. 2022;12:10612.
7. Giorgetti A, Baldanzini N, Biasiotto M, Citti P. Design and testing of a MRF rotational damper for vehicle applications. Smart Materials and Structures. 2010;19(6):065006.
8. Li DD, Keogh DF, Huang K, Chan QN, Yuen ACY, Menictas C et al. Modeling the response of magnetorheological fluid dampes under seismic conditions.
9. Kubík M, Macháček O, Strecker Z, Roupec J, Mazůrek I. Design and testing of magnetorheological valve with fast force response time and great dynamic force range. Smart Materials and Structures. 2017;26(4):047002.
10. Thakur MK, Sarkar C. Experimental and numerical study of magnetorheological clutch with sealing at larger radius disc. Defence Science Journal. 2020;70(6):575-582.
11. Patel S, Upadhyay R, Patel D. Design optimization of magnetorheological brake using structural parameter: evaluation and validation. IOP Conference Series: Materials Science and Engineering. 2020;992:012004.
12. Horak W. Modeling of magnetorheological fluid in quasi-static squeeze flow mode. Smart Materials and Structures. 2018; 27: 065022.
13. Sapiński B, Gołdasz J. Development and performance evaluation of an MR squeeze-mode damper. Smart Materials and Structures. 2015;24(11):115007.
14. Sapiński B, Rosół M, Jastrzębski Ł, Gołdasz J. Outlook on the dynamic behavior of an magnetorheological squeeze-mode damper prototype. Journal of Intelligent Material Systems and Structures. 2017;28(20):3025-3038.
15. Goncalves FD, Carlson JD. An alternate operation mode for MR fluids – Magnetic Gradient Pinch. Journal of Physics: Conference Series. 2009;149:012050.
16. Gołdasz J, Sapiński B. Magnetostatic analysis of a pinch mode magnetorheological valve. Acta Mechanica et Automatica. 2017;11(3):229-232.
17. Sapiński B, Horak W. Rheological properties of MR fluids recommended for use in shock absorbers. Acta Mechanica et Automatica. 2013;7(2):107-110.
18. Quoc NV, Tuan LD, Hiep LD, Quoc HN, Choi SB. Material characterization of MR fluid on performance of MRF based brake. Frontiers in Materials. 2019; 6: 125.
19. Lokhande SB, Patil SR. Experimental characterization and evaluation of magnetorheological clutch for an electric two-wheeler application. Measurement. 2021;175:109150.
20. Strecker Z, Jeniš F, Kubík M, Macháček O, Choi SB. Novel approaches to the design of an ultra-fast magnetorheological valve for semi-active control. Materials. 2021;14(10):2500.
21. Gołdasz J, Sapiński B, Kubík M, Macháček O, Bańkosz W et al. Review: a survey on configurations and performance of flow-mode MR valves. Applied Sciences. 2022;12(12):6260.
22. Laun H.M, Gabril C, Kieburg Ch. Twin gap magneorheometer using ferromagnetic steel plates – Performance and validation. Journal of Rheology. 2010;54:327-354.
23. Wang K, Dong X, Li J, Shi K. Yield dimensionless magnetic effect and shear thinning for magnetorheological grease. Results in Physics. 2020;18:103328.
24. Han S, Choi J, Han HN, Kim S, Seo Y. Effect of particle shape anisotropy on the performance and stability of magnetorheological fluids. ACS Applied Electronic Materials. 2021;3:2526-2533.
25. Jeon J, Koo S. Viscosity and dispersion state of magnetic suspensions. Journal of Magnetism and Magnetic Materials. 2012;324: 424-429.
26. Nagdeve L, Sidpara A, Jain VK, Ramkumar J. On the effect of relative size of magnetic particles and abrasive particles in MR fluid-based finishing process. Machining Science and Technology. 2018;22(3):493-506.
27. Acharya S, Tak RSS, Singh SB, Kumar H. Characterization of magnetorheological brake utilizing synthesized and commercial fluids. Materials Today: Procedings. 2021;46(19):9419-9424.
28. Mezger TG. The Rheology Handbook. 4th edition. Hanover: Vincentz Network GmbH & Co; 2014.
29. Elsaady W, Oyadiji SO, Nasser A. A review on multi-physics numerical modelling in different applications of magnetorheological fluids. Journal of Intelligent Systems and Structures. 2020;31(16):1855-1897.
30. Chaudhuri A, Wereley NM, Radhakrishnan R, Choi SB. Rheological parameter estimation for a ferrous nanoparticle-based magnetorheological fluid using genetic algorithms. Journal of Intelligent Material Systems and Structures. 2006;17(3):261-269.
31. Laun HM, Gabriel C, Kieburg C. Magnetorheological fluid (MRF) in oscillatory shear and parametrization with regard to MR device properties. Journal of Physics: Conference Series. 2009;149:012067.
32. Wereley NM, Chaudhuri A, Yoo J-H, John S, Kotha S, Suggs A et al. Bidisperse magnetorheological fluids using Fe particles at nanometer and micron scale. Journal of Intelligent Material Systems and Structures. 2006;17(5):393-401.
33. LORD Corporation. MRF-132DG Magneto-Rheological Fluid. DS7015 datasheet [Internet]. 2011 Nov [cited 2022 Jul 15]. Available from: https://lordfulfillment.com/pdf/44/DS7015_MRF-132DGMRFluid.pdf
34. Barnes HA. The yield stress – a review or 'παντα ρει'—everything flows? Journal of Non-Newtonian Fluid Mechanics. 1999;81 (1-2):133-178.
35. Ichwan B, Mazlan SA, Imaduddin F, Ubaidillah, Zamzuri H. Performance simulation on a magnetorheological valve module using three different commercial magnetorheological fluid. Advanced Materials Research. 2015;1123:35-41.
36. Szakal RA, Susan-Resiga D, Muntean S, Ladislau V. Magnetorheological fluids flow modelling used in a magnetorheological brake configuration. 2019 International Conference on ENERGY and ENVIRONMENT (CIEM). 2019:403-407.
37. Szakal RA, Mecea D, Bosioc AI, Borbáth I, Muntean S. Design and testing a magneto-rheological brake with cylindrical configuration. Proceeding of the Romanian Academy – Series A: Mathematics, Physics, Technical Sciences, Information Science. 2021;22(2/2021):189-197.

Wojciech Horak: https://orcid.org/0000-0002-2258-4233

Barbara Stępień: https://orcid.org/0000-0001-7802-4342

Bogdan Sapiński: https://orcid.org/0000-0001-6952-8303